Observation of an Odd-Integer Quantum Hall Effect from Topological Surface States in Cd_3As_2

Ben-Chuan Lin,[1,*] Shuo Wang,[1,*] Steffen Wiedmann,[2,3] Jian-Ming Lu,[1,2] Wen-Zhuang Zheng,[1] Dapeng Yu,[4] and Zhi-Min Liao[1,5,6,†]

[1]*State Key Laboratory for Mesoscopic Physics, School of Physics, Peking University, Beijing 100871, China*
[2]*High Field Magnet Laboratory (HFML-EMFL), Radboud University, Toernooiveld 7, Nijmegen 6525 ED, Netherlands*
[3]*Radboud University, Institute for Molecules and Materials, Nijmegen 6525 AJ, Netherlands*
[4]*Institute for Quantum Science and Engineering and Department of Physics, South University of Science and Technology of China, Shenzhen 518055, China*
[5]*Beijing Key Laboratory of Quantum Devices, Peking University, Beijing 100871, China*
[6]*Collaborative Innovation Center of Quantum Matter, Beijing 100871, China*

(Received 1 November 2018; published 25 January 2019)

The quantum Hall effect (QHE) in a 3D Dirac semimetal thin film is attributed to either the quantum confinement induced bulk subbands or the Weyl orbits that connect the opposite surfaces via bulk Weyl nodes. However, it is still unknown whether the QHE based on the Weyl orbit can survive as the bulk Weyl nodes are gapped. Moreover, there are closed Fermi loops rather than open Fermi arcs on the Dirac semimetal surface, which can also host the QHE. Here we report the QHE in the 3D Dirac semimetal Cd_3As_2 nanoplate by tuning the gate voltage under a fixed 30 T magnetic field. The quantized Hall plateaus at odd filling factors are observed as a magnetic field along the [001] crystal direction, indicating a Berry's phase π from the topological surface states. Furthermore, even filling factors are observed when the magnetic field is along the [112] direction, indicating the C_4 rotational symmetry breaking and a topological phase transition. The results shed light on the understanding of QHE in 3D Cd_3As_2.

DOI: 10.1103/PhysRevLett.122.036602

The three-dimensional (3D) Dirac semimetal Cd_3As_2 has linear energy dispersion in bulk states and topologically protected surface states [1–19]. This protection is due to the C_4 rotation symmetry that prohibits a gap near the Dirac point [1,2]. Lots of interesting transport properties have been revealed in 3D Dirac semimetals, such as chiral anomaly induced negative magnetoresistance [9,10], Weyl-orbit related quantum oscillations [13,14], Berry's phase π related Aharonov-Bohm effect [15,16], bulk-surface interference induced Fano effect [19], etc. Furthermore, the quantum Hall effect (QHE) in Cd_3As_2 films has been reported recently [20–23]. For Dirac materials, the quantum Hall plateaus are generally observed at $g \times (n + 1/2)e^2/h$, where g is the degeneracy and the $1/2$ term comes from the Berry's phase π [24]. For monolayer graphene, the $g \sim 4$ comes from the spin and valley degrees [24], and thus the filling factors were found at $\upsilon = 2, 6, 10, \ldots$. For topological insulators, the degeneracy stems from top and bottom surfaces and thus the filling factors $\upsilon = (n_t + \frac{1}{2}) + (n_b + \frac{1}{2}) = n_t + n_b + 1$, where $n_{t(b)}$ is the Landau level index of the top (bottom) surface [25]. Thus, the filling factors can be a series of continuous integer values (both odd and even) or only odd series depending on the top and bottom surface carrier densities [25]. However, the quantum Hall plateaus in Cd_3As_2 were found to be a series of even filling factors $\upsilon = 1, 2, 4, 6$, where $\upsilon = 1$ is attributed to the splitting of the lowest Landau level [21,22]. Nishihaya *et al.* attributed the observed QHE to the quantum confinement induced bulk subbands in the thin film with thickness ~35 nm [20,22]. Schumann *et al.* proposed that the QHE may from the Weyl orbit for the same film thickness ~35 nm [21]. Despite the debate on the mechanism of the QHE, the quantum Hall plateaus at even filling factors $g \times ne^2/h$ with $g \sim 2$ indicate the absence of the Berry's phase π or the topological nature [22].

In this work, we report the observations of the quantum Hall plateaus at odd filling factors $\upsilon = 1, 3, 5$ under a tilted magnetic field along the [001] crystal direction, besides previously reported filling factors $\upsilon = 1, 2, 4, 6$ under a perpendicular magnetic field along the [112] direction. The evolution of the quantum Hall plateaus with the magnetic field direction cannot be explained by the bulk subbands scenario or the Weyl-orbit theory. Instead, it is consistent with the topological surface states of the 3D Dirac semimetals.

A typical device of the Cd_3As_2 nanoplates is shown by the scanning electron microscopy image in Fig. 1(a). The high crystal quality nanoplates with (112) surface plane were grown by chemical vapor deposition (CVD) method [10,26] and then transferred to a silicon substrate with a layer of 285 nm SiO_2. The nanoplate thickness is ~80 nm

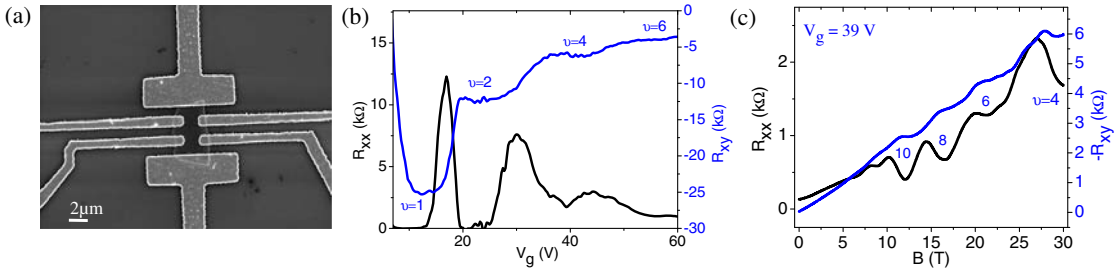

FIG. 1. (a) SEM image of a typical Cd_3As_2 nanoplate Hall-bar device. (b) The R_{xx} and R_{xy} vs V_g measured under a perpendicular magnetic field of 30 T. The gate voltage was applied on the silicon substrate with a layer of 285 nm SiO_2. (c) The SdH oscillations of R_{xx} and the corresponding R_{xy} at $V_g = 39$ V.

and gold electrodes were deposited immediately after Ar^+ ion etching process to form Ohmic contacts. Figure 1(b) shows the longitudinal resistance (R_{xx}) and transverse resistance (R_{xy}) measured at 1.5 K as a function of back gate voltage (V_g) under the perpendicular magnetic field $B \sim 30$ T. With such a high magnetic field, the Landau levels are fully developed and the plateaus at filling factors $\upsilon = 1, 2, 4, 6$ were clearly observed. Particularly, the R_{xx} reaches zero at R_{xy} plateaus with filling factors $\upsilon = 1, 2$, which shows an exact 2D QHE. The magnetic field dependence of R_{xx} and R_{xy} at $V_g = 39$ V are presented in Fig. 1(c). A series of plateaus at filling factors $\upsilon = 4, 6, 8, 10$ were also observed. Such a series of quantum Hall plateaus at even filling factors are consistent with previous experiments [21,22].

Figure 2(a) shows the R_{xy} evolution with the angle θ, defined as the angle between the magnetic field orientation and the normal direction of the substrate, under fixed magnetic field 30 T. As we gradually rotate the magnetic field towards the [001] direction ($\theta = 54.7°$), namely the C_4 rotation symmetry axis, the plateaus gradually transform from $\upsilon = 2, 4, 6$ to $\upsilon = 3, 5$. The plateau widths represented by gate voltage were extracted from the V_g dependence of both R_{xy} and dR_{xy}/dV_g curves under 30 T, as presented in Fig. 2(b). With increasing θ, namely, the magnetic field direction closer to the [001] direction, the plateau width gradually diminishes at $\upsilon = 2$, 4 while is prominent at $\upsilon = 3$. Figure 2(c) presents the flow of conductivity tensor (σ_{xy}, σ_{xx}) at $\theta = 0°$ and 54.7°, which allows the extraction of two converging points in the (σ_{xy}, σ_{xx}) space [27,28]. The quantized σ_{xy} with vanishing σ_{xx} would be presented as a curve dip, as shown in the inset of Fig. 2(c). The dips in Fig. 2(c) are found at $\upsilon = 2, 4, 6$ for $\theta = 0°$ ($\boldsymbol{B}$ along the [112] direction) and at $\upsilon = 1, 3, 5$ for $\theta = 54.7°$ ($\boldsymbol{B}$ along the [001] direction). As for $\theta = 42°$, near the [001] direction, Fig. 2(d) shows the dR_{xy}/dV_g and the corresponding R_{xx} under 30 T. At the R_{xy} plateaus, the dR_{xy}/dV_g is near zero and the R_{xx} also shows a resistance dip. The results indicate that quantum Hall plateaus with odd series were developed under the tilted magnetic field near the [001] crystal direction.

The Landau levels formation was further analyzed through temperature dependent measurements. Figures 3(a) and 3(b) show the temperature evolution of R_{xx} under $B \sim 30$ T with $\theta = 0°$ (the [112] direction) and $\theta = 42°$ (near the [001] direction), respectively. For $\theta = 0°$, the $\upsilon = 2$ state is still clearly observed at 60 K. While for $\theta = 42°$, the $\upsilon = 1$ state is still clearly observed at 42 K. The Landau level gap can be extracted through the Arrhenius plot, i.e., $\ln(R_{xx})$ vs T^{-1} curve. As shown in Fig. 3(c), the Landau level gaps (Δ) are 48.9, 33.2, and 0.78 K at $\theta = 0°$ for $\upsilon = 1, 2, 4$, respectively. While for $\theta = 42°$, Δ is 33.1, 4.8, and 0.88 K for $\upsilon = 1$, 2, 3, respectively, as shown in Fig. 3(d). Apparently the $\Delta_{\upsilon=2}$ at $\theta = 42°$ is nearly an order of magnitude smaller than that at $\theta = 0°$, suggesting that

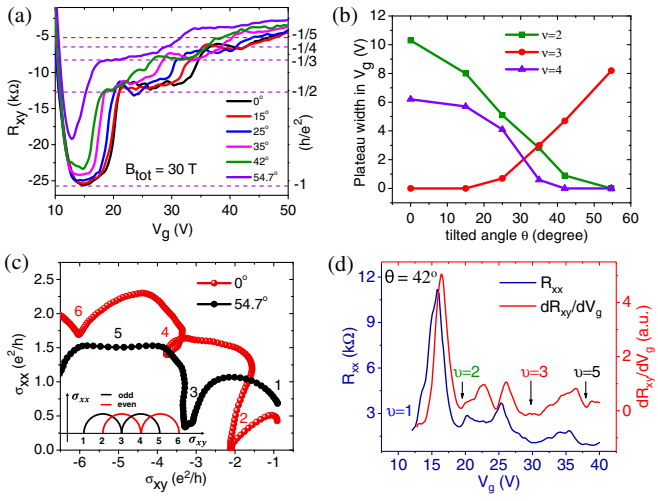

FIG. 2. (a) The quantum Hall plateaus in R_{xy} vs V_g under a rotated magnetic field of 30 T from $\theta = 0°$ (perpendicular to the substrate) to 54.7° (along the [001] crystal direction). (b) The width of quantum Hall plateau extracted from (a), which is defined in units of V_g. From $\theta = 0°$ to 54.7°, the filling factors $\nu = 2$, 4 gradually decays and $\nu = 3$ emerges. (c) The flow analysis of the transverse and longitudinal conductance at $\theta = 0°$ and 54.7°. Inset: The theoretical flow of conductivity tensor (σ_{xy}, σ_{xx}) for the odd and even integer QHE, respectively. (d) The SdH oscillations of R_{xx} and the corresponding dR_{xy}/dV_g at $\theta = 42°$. It is evident that the plateaus at $\nu = 3$, 5 emerge.

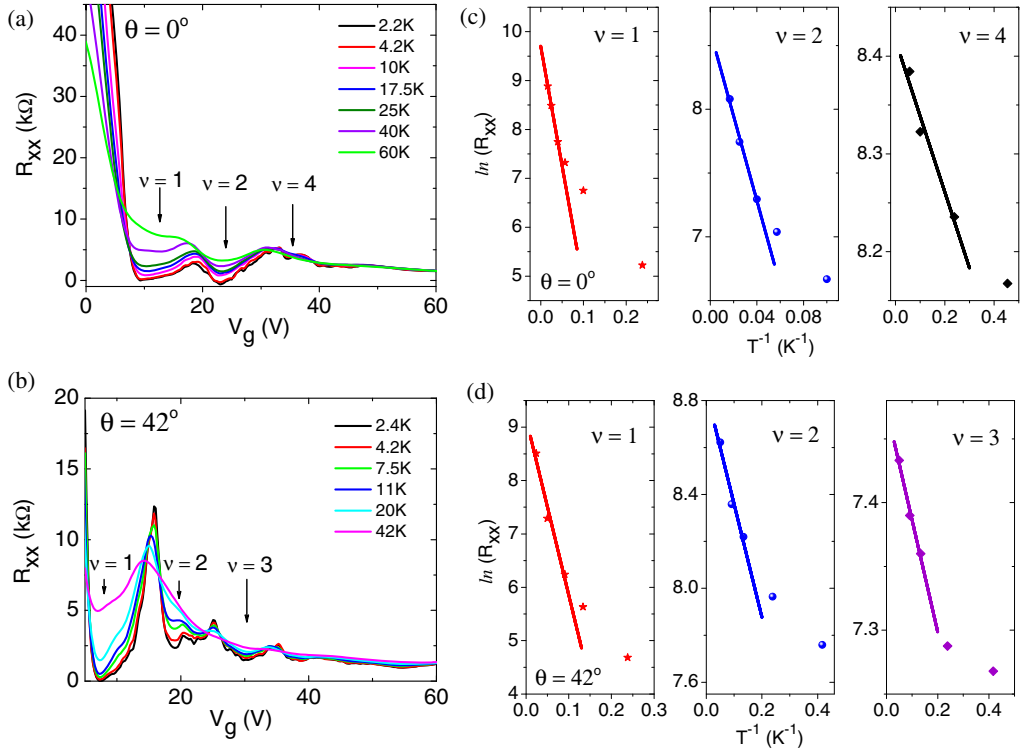

FIG. 3. (a),(b) Under 30 T, the temperature evolution of R_{xx} vs V_g at $\theta = 0°$ and 42°, respectively. (c),(d) The Arrhenius plot of the temperature dependence of R_{xx}. From the $\ln(R_{xx}) \sim T^{-1}$ linear fittings, the Landau level gaps were extracted. Here $\ln(R_{xx})$ is calculated from R_{xx} in Ohms.

$\upsilon = 2$ mainly comes from the lowest Landau level splitting for B near the [001] crystal direction. In contrast, the $\Delta_{\upsilon=3}$ at $\theta = 42°$ is comparable to the $\Delta_{\upsilon=4}$ at $\theta = 0°$. Therefore, besides the lowest Landau level splitting, the dominate filling factors are $\upsilon = 2, 4, 6$ for $\theta = 0°$ and $\upsilon = 1, 3, 5$ for $\theta = 42°$.

The observed quantum Hall effect at $g \times (n + 1/2)e^2/h$ is a manifestation of Berry's phase π associated with spin-helical carriers of the surface states [24,25]. In previous literature, the missing $1/2$ term under perpendicular magnetic field is attributed to the quantum confinement induced subband gap near the Dirac point [22]. Considering the degeneracy $g \sim 2$, only even plateaus were observed. The $\nu = 1$ plateau is further explained by the splitting of the lowest Landau level [22] or other orbit related effects [29]. However, such a subband scenario cannot explain our experiments, because the subband gap induced by the dimension confinement would always exist no matter what the magnetic field direction is.

The experimental results can be understood by considering the C_4 rotation symmetry with the magnetic field direction. When the magnetic field is along the [001] crystal direction, the C_4 symmetry would not be influenced. The Landau levels are $\mathrm{E} = \hbar v_F \mathrm{sgn}(n)\sqrt{(2|n|eB/\hbar) + (\boldsymbol{k}\cdot\boldsymbol{b})^2}$, with $n = \pm 1, \pm 2, \ldots$, where v_F is the Fermi velocity and $\boldsymbol{b}$ is the unit denoting the magnetic field direction [9,30], as shown in Fig. 4(a). For the $n = 0$ Landau level, there are linear dispersions $E_0 = \pm\hbar v_F \boldsymbol{k}\cdot\boldsymbol{b}$. In this situation, the topological surface states are Fermi loops formed by two Fermi arcs that connect the projections of Dirac nodes on the surface [31,32]. The nontrivial Fermi-loop surface states may be responsible for the observed odd-integer QHE.

However, when the magnetic field is along the [112] crystal direction, which has a large deviation from the C_4 rotation symmetry axis, the C_4 rotation symmetry would be broken [2,29], leading to a gap near the Dirac point, as shown in Fig. 4(b). Thus the $n = 0$ Landau level with linear dispersion would be missing. The crystal symmetry breaking term would mix the two Fermi arcs and reconstruct the

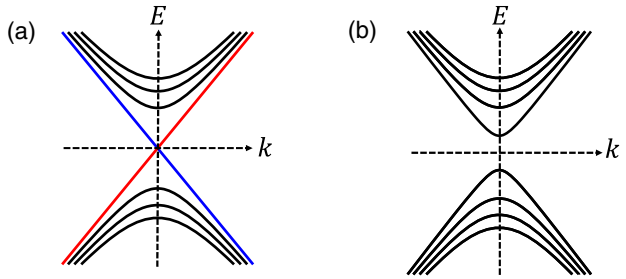

FIG. 4. (a) Landau levels with C_4 rotation symmetry preserved under strong magnetic field. The $n = 0$ Landau level has linear dispersion. The red and blue lines denote different chiralities. (b) Landau levels without C_4 rotation symmetry. A gap is opened near Dirac point.

surface states [13], leading to a trivial state. Thus the even integer QHE can be observed. On the other hand, quantum confinement induced bulk subbands can also host the even integer QHE [20,22]. It is not easy to identify whether the even integer QHE comes from the bulk subbands or trivial surface states under a perpendicular magnetic field. For our experiments, the observation of the topological phase transition rules out the bulk subbands origination. It should be noticed that our sample is not too thin to induce the hybridization of the top and bottom surfaces [2], which prevents the bulk gap opening in all three dimensions. Our sample is also not so thick that the bulk states become continuous along the thickness direction. Otherwise, no QHE could be observed.

Furthermore, the Weyl orbit interpretation is not suitable for our experimental results. The 3D quantum Hall effect formed by Weyl orbits was predicated in Cd_3As_2, using a sort of model Hamiltonian in which the effect of C_4 rotational symmetry breaking is not explicitly implemented [17]. However, it remains a question whether the QHE based on the Weyl orbit can still survive as the bulk Weyl nodes are gapped. The "wormhole" tunneling via the bulk Weyl nodes may be blocked, as the gapped Weyl nodes are not the singular points in both energy and momentum spaces [29]. On the other hand, the closed Fermi loops can be formed at one surface of Dirac semimetal Cd_3As_2 rather than just open Fermi arcs. Therefore, our observed odd-filling QHE is more likely to be attributed to the topological surface Fermi loops rather than the Weyl orbits.

In summary, we have observed both odd and even integer QHE in Cd_3As_2 nanoplates through tuning gate voltage under a rotational 30 T magnetic field. The quantum Hall plateau evolution indicates a topological phase transition of the surface states when the C_4 rotational symmetry is broken by magnetic field. Besides the previously reported bulk subbands and Weyl orbit scenarios, the topological surface states with Fermi loops provide another mechanism for the QHE in 3D Dirac semimetals. Our results shed light on understanding the topological properties and QHE of the 3D Dirac semimetals.

This work was supported by NSFC (No. 61825401 and No. 11774004), and National Key Research and Development Program of China (No. 2016YFA0300802). We acknowledge the support of the High Field Magnet Laboratory (HFML) in Nijmegen, member of the European Magnetic Field Laboratory (EMFL).

Note added in proof.—We became aware of Ref. [33], which claimed a QHE based on Weyl orbits according to the phase shift with the thickness variations in a wedge-shaped Cd_3As_2 nanoplate. However, such a phase shift may also come from bulk subbands, because the quantum confinement is accordingly altered with different thickness [also see the Figs. 2(c)–2(d) in Ref. [20]]. On the other hand, the CVD-grown wedge-shaped sample is not homogeneous in thickness and also in carrier density [the slopes of R_{xy}^{1-2} and R_{xy}^{5-6} curves are different in the magnetic field range from 0 to 5 T in Fig. 2(e) in Ref. [33]], which can also cause the shift of the Hall plateaus.

*These authors contributed equally to this work.
†liaozm@pku.edu.cn

[1] S. M. Young, S. Zaheer, J. C. Y. Teo, C. L. Kane, E. J. Mele, and A. M. Rappe, Dirac Semimetal in Three Dimensions, Phys. Rev. Lett. **108**, 140405 (2012).
[2] Z. Wang, H. Weng, Q. Wu, X. Dai, and Z. Fang, Three-dimensional Dirac semimetal and quantum transport in Cd_3As_2, Phys. Rev. B **88**, 125427 (2013).
[3] S. Borisenko, Q. Gibson, D. Evtushinsky, V. Zabolotnyy, B. Büchner, and R. J. Cava, Experimental Realization of a Three-Dimensional Dirac Semimetal, Phys. Rev. Lett. **113**, 027603 (2014).
[4] Z. K. Liu, J. Jiang, B. Zhou, Z. J. Wang, Y. Zhang, H. M. Weng, D. Prabhakaran, S.-K. Mo, H. Peng, P. Dudin, T. Kim, M. Hoesch, Z. Fang, X. Dai, Z. X. Shen, D. L. Feng, Z. Hussain, and Y. L. Chen, A stable three-dimensional topological Dirac semimetal Cd_3As_2, Nat. Mater. **13**, 677 (2014).
[5] M. Neupane, S.-Y. Xu, R. Sankar, N. Alidoust, G. Bian, C. Liu, I. Belopolski, T.-R. Chang, H.-T. Jeng, H. Lin, A. Bansil, F. Chou, and M. Z. Hasan, Observation of a three-dimensional topological Dirac semimetal phase in high-mobility Cd_3As_2, Nat. Commun. **5**, 3786 (2014).
[6] H. Yi, Z. Wang, C. Chen, Y. Shi, Y. Feng, A. Liang, Z. Xie, S. He, J. He, Y. Peng, X. Liu, Y. Liu, L. Zhao, G. Liu, X. Dong, J. Zhang, M. Nakatake, M. Arita, K. Shimada, H. Namatame *et al.*, Evidence of topological surface state in three-dimensional Dirac semimetal Cd_3As_2, Sci. Rep. **4**, 6106 (2014).
[7] S.-Y. Xu, C. Liu, S. K. Kushwaha, R. Sankar, J. W. Krizan, I. Belopolski, M. Neupane, G. Bian, N. Alidoust, T.-R. Chang, H.-T. Jeng, C.-Y. Huang, W.-F. Tsai, H. Lin, P. P. Shibayev, F.-C. Chou, R. J. Cava, and M. Z. Hasan, Observation of Fermi arc surface states in a topological metal, Science **347**, 294 (2015).
[8] H.-J. Kim, K.-S. Kim, J.-F. Wang, M. Sasaki, N. Satoh, A. Ohnishi, M. Kitaura, M. Yang, and L. Li, Dirac versus Weyl Fermions in Topological Insulators: Adler-Bell-Jackiw Anomaly in Transport Phenomena, Phys. Rev. Lett. **111**, 246603 (2013).
[9] J. Xiong, S. K. Kushwaha, T. Liang, J. W. Krizan, M. Hirschberger, W. D. Wang, R. J. Cava, and N. P. Ong, Evidence for the chiral anomaly in the Dirac semimetal Na_3Bi, Science **350**, 413 (2015).
[10] C.-Z. Li, L.-X. Wang, H. Liu, J. Wang, Z.-M. Liao, and D.-P. Yu, Giant negative magnetoresistance induced by the chiral anomaly in individual Cd_3As_2 nanowires, Nat. Commun. **6**, 10137 (2015).
[11] T. Liang, Q. Gibson, M. N. Ali, M. Liu, R. J. Cava, and N. P. Ong, Ultrahigh mobility and giant magnetoresistance in the Dirac semimetal Cd_3As_2, Nat. Mater. **14**, 280 (2015).

[12] A. Narayanan, M. D. Watson, S. F. Blake, N. Bruyant, L. Drigo, Y. L. Chen, D. Prabhakaran, B. Yan, C. Felser, T. Kong, P. C. Canfield, and A. I. Coldea, Linear Magnetoresistance Caused by Mobility Fluctuations in n-Doped Cd_3As_2, Phys. Rev. Lett. **114**, 117201 (2015).

[13] A. C. Potter, I. Kimchi, and A. Vishwanath, Quantum oscillations from surface Fermi arcs in Weyl and Dirac semimetals, Nat. Commun. **5**, 5161 (2014).

[14] P. J. W. Moll, N. L. Nair, T. Helm, A. C. Potter, I. Kimchi, A. Vishwanath, and J. G. Analytis, Transport evidence for Fermi-arc-mediated chirality transfer in the Dirac semimetal Cd_3As_2, Nature (London) **535**, 266 (2016).

[15] B.-C. Lin, S. Wang, L.-X. Wang, C.-Z. Li, J.-G. Li, D. Yu, and Z.-M. Liao, Gate-tuned Aharonov-Bohm interference of surface states in a quasiballistic Dirac semimetal nanowire, Phys. Rev. B **95**, 235436 (2017).

[16] L.-X. Wang, C.-Z. Li, D.-P. Yu, and Z.-M. Liao, Aharonov-Bohm oscillations in Dirac semimetal Cd_3As_2 nanowires, Nat. Commun. **7**, 10769 (2016).

[17] C. M. Wang, H.-P. Sun, H.-Z. Lu, and X. C. Xie, 3D Quantum Hall Effect of Fermi Arcs in Topological Semimetals, Phys. Rev. Lett. **119**, 136806 (2017).

[18] S. Wang, B.-C. Lin, A.-Q. Wang, D.-P. Yu, and Z.-M. Liao, Quantum transport in Dirac and Weyl semimetals: a review, Adv. Phys. X **2**, 518 (2017).

[19] S. Wang, B.-C. Lin, W.-Z. Zheng, D. Yu, and Z.-M. Liao, Fano Interference between Bulk and Surface States of a Dirac Semimetal Cd_3As_2 Nanowire, Phys. Rev. Lett. **120**, 257701 (2018).

[20] M. Uchida, Y. Nakazawa, S. Nishihaya, K. Akiba, M. Kriener, Y. Kozuka, A. Miyake, Y. Taguchi, M. Tokunaga, N. Nagaosa, Y. Tokura, and M. Kawasaki, Quantum Hall states observed in thin films of Dirac semimetal Cd_3As_2, Nat. Commun. **8**, 2274 (2017).

[21] T. Schumann, L. Galletti, D. A. Kealhofer, H. Kim, M. Goyal, and S. Stemmer, Observation of the Quantum Hall Effect in Confined Films of the Three-Dimensional Dirac Semimetal Cd_3As_2, Phys. Rev. Lett. **120**, 016801 (2018).

[22] S. Nishihaya, M. Uchida, Y. Nakazawa, M. Kriener, Y. Kozuka, Y. Taguchi, and M. Kawasaki, Gate-tuned quantum Hall states in Dirac semimetal $(Cd_{1-x}Zn_x)_3As_2$, Sci. Adv. **4**, eaar5668 (2018).

[23] C. Zhang, A. Narayan, S. Lu, J. Zhang, H. Zhang, Z. Ni, X. Yuan, Y. Liu, J.-H. Park, E. Zhang, W. Wang, S. Liu, L. Cheng, L. Pi, Z. Sheng, S. Sanvito, and F. Xiu, Evolution of Weyl orbit and quantum Hall effect in Dirac semimetal Cd_3As_2, Nat. Commun. **8**, 1272 (2017).

[24] A. H. Castro Neto, F. Guinea, N. M. R. Peres, K. S. Novoselov, and A. K. Geim, The electronic properties of graphene, Rev. Mod. Phys. **81**, 109 (2009).

[25] Y. Xu, I. Miotkowski, C. Liu, J. Tian, H. Nam, N. Alidoust, J. Hu, C.-K. Shih, M. Z. Hasan, and Y. P. Chen, Observation of topological surface state quantum Hall effect in an intrinsic three-dimensional topological insulator, Nat. Phys. **10**, 956 (2014).

[26] C.-Z. Li, J.-G. Li, L.-X. Wang, L. Zhang, J.-M. Zhang, D. Yu, and Z.-M. Liao, Two-carrier transport induced Hall anomaly and large tunable magnetoresistance in Dirac semimetal Cd_3As_2 nanoplates, ACS Nano **10**, 6020 (2016).

[27] R. Yoshimi, A. Tsukazaki, Y. Kozuka, J. Falson, K. S. Takahashi, J. G. Checkelsky, N. Nagaosa, M. Kawasaki, and Y. Tokura, Quantum Hall effect on top and bottom surface states of topological insulator $(Bi_{1-x}Sb_x)_2Te_3$ films, Nat. Commun. **6**, 6627 (2015).

[28] S. Zhang, L. Pi, R. Wang, G. Yu, X.-C. Pan, Z. Wei, J. Zhang, C. Xi, Z. Bai, F. Fei, M. Wang, J. Liao, Y. Li, X. Wang, F. Song, Y. Zhang, B. Wang, D. Xing, and G. Wang, Anomalous quantization trajectory and parity anomaly in Co cluster decorated $BiSbTeSe_2$ nanodevices, Nat. Commun. **8**, 977 (2017).

[29] S. Jeon, B. B. Zhou, A. Gyenis, B. E. Feldman, I. Kimchi, A. C. Potter, Q. D. Gibson, R. J. Cava, A. Vishwanath, and A. Yazdani, Landau quantization and quasiparticle interference in the three-dimensional Dirac semimetal Cd_3As_2, Nat. Mater. **13**, 851 (2014).

[30] S. A. Parameswaran, T. Grover, D. A. Abanin, D. A. Pesin, and A. Vishwanath, Probing the Chiral Anomaly with Nonlocal Transport in Three-Dimensional Topological Semimetals, Phys. Rev. X **4**, 031035 (2014).

[31] B.-J. Yang and N. Nagaosa, Classification of stable three-dimensional Dirac semimetals with nontrivial topology, Nat. Commun. **5**, 4898 (2014).

[32] S. Kobayashi and M. Sato, Topological Superconductivity in Dirac Semimetals, Phys. Rev. Lett. **115**, 187001 (2015).

[33] C. Zhang, Y. Zhang, X. Yuan, S. Lu, J. Zhang, A. Narayan, Y. Liu, H. Zhang, Z. Ni, R. Liu, E. S. Choi, A. Suslov, S. Sanvito, L. Pi, H.-Z. Lu, A. C. Potter, and F. Xiu, Quantum Hall effect based on Weyl orbits in Cd_3As_2, Nature (London) **565**, 331 (2019).